Regeneration of CuO-ZnO-Al$_2$O$_3$/γ-Al$_2$O$_3$ catalyst in the direct synthesis of dimethyl ether

Irene Sierra, Javier Ereña [*], Andrés T. Aguayo, José M. Arandes, Javier Bilbao

Departamento de Ingeniería Química, Universidad del País Vasco, Apartado 644, E-48080 Bilbao, Spain

A B S T R A C T

This paper deals with the regeneration of a CuO-ZnO-Al$_2$O$_3$/γ-Al$_2$O$_3$ catalyst used in the direct synthesis of dimethyl ether. When coke combustion (subsequent to aging treatment) is performed in a thermobalance, two coke fractions with different combustion kinetics are identified. One coke fraction, deposited on the metallic sites and whose combustion is activated by these sites, has a kinetic constant of combustion 7–26 times higher than that corresponding to the coke located at the Al$_2$O$_3$ support. Uninterrupted operation is feasible in reaction–regeneration cycles in a fixed bed reactor as long as the reaction and regeneration steps are carried out at 325 °C, which are limiting conditions in order to avoid irreversible deactivation by sintering of the metallic function. The regeneration with O$_2$ diluted with He (5% of O$_2$) allows the complete combustion of coke. Under conditions of partial coke combustion it is observed that the removal of the fraction deposited on the metal makes it possible to recover the initial activity of the catalyst, which subsequently undergoes fast deactivation.

© 2009 Elsevier B.V. All rights reserved.

1. Introduction

The synthesis of dimethyl ether (DME) from syngas in one reaction step using a bifunctional catalyst (STD process) has advantages over the two-step process (methanol synthesis and its dehydration to DME), since the thermodynamic limitation is reduced, which allows using higher temperatures and lower pressures than those corresponding to methanol synthesis [1,2].

The increasing interest in the industrial implementation of the STD process is also explained by the development of DME applications. It is an environmentally friendly fuel (sulfur-free and with a low particle and NO$_x$ emission), which can replace LPG as a domestic fuel, and can be used as a gasoline additive and automotive diesel [3–6]. Furthermore, DME is an intermediate raw material (alternative to methanol) for the production of hydrocarbons (light olefins, BTXE, conventional fuels), chemicals (dimethyl sulphate, methyl acetate) and H$_2$, by means of the steam catalytic reforming [7–11]. Furthermore, its low toxicity and average lifetime in the atmosphere (approximately 5 days), make it possible to use DME as an aerosol propellant, replacing chlorofluorocarbons (CFCs) [12].

The bifunctional catalyst for the STD process is made up of a metallic phase that is active for methanol synthesis (the most frequently used function is CuO-ZnO-Al$_2$O$_3$ with different component ratios and with additives such as Mn and ZrO$_2$), and an acidic

function that is active for the dehydration of methanol and selective for the synthesis of DME, which requires a moderate acid strength to minimize hydrocarbon production reactions from DME (more active than methanol). The most commonly used acidic functions are γ-Al$_2$O$_3$ [13–17] and HZSM-5 zeolite (with a high Si/Al ratio or partially sodic) [18,19], although other microporous zeolites with moderate acidity have also been used [20–23].

Catalyst deactivation has been scarcely studied in the literature, and even less its regeneration, which is a key factor for the viability of the process. Cu sintering and mainly coke deposition [16,24–26] have been identified as the possible causes of catalyst deactivation. Attention has also been paid to the attenuation of catalyst activity by water adsorption, enhanced by the hydrophilic nature of both Al$_2$O$_3$, support of the metallic function, and the γ-Al$_2$O$_3$ acidic function, which has a significant water adsorption capacity [16].

In a previous work, the origin of the deactivation of CuO-ZnO-Al$_2$O$_3$/γ-Al$_2$O$_3$ catalyst has been studied, which is mainly attributed to coke deposition. This conclusion is based on the study of the evolution with time on stream of the properties of metallic and acidic functions, as well as coke evolution, determined from the oxidation at programmed temperature (TPO curves) [27]. Based on the results it is concluded that coke has presumably its origin in the degradation of reaction intermediates (methoxy groups), and evolves towards high molecular weight structures through the known mechanisms of oligomerization, cyclization and condensation [28]. Coke initially blocks the metallic sites, but as it grows the carbonaceous material is deposited on Al$_2$O$_3$ support pores. Coke deposition on the acidic function begins to be noticeable for high values of time on stream. In any case, since the

---

Nomenclature

C_1	concentration of the coke fraction deposited on CuO-ZnO sites of the catalyst, g (g of catalyst)$^{-1}$
C_2	concentration of the coke fraction deposited on the Al$_2$O$_3$ support, g (g of catalyst)$^{-1}$
DME	dimethyl ether
E_i	activation energy corresponding to the combustion of i coke, kJ mol^{-1}
k_i, $k_{ref,i}$	kinetic constant for the combustion of i coke and its value at the reference temperature (250 °C), bar^{-1} s^{-1}
LPG	liquefied petroleum gas
$(n_{CO})_0$	molar flowrate of CO in the feed, mol s^{-1}
n_{DME}	molar flowrate of DME in the product stream, mol s^{-1}
P_{O_2}	partial pressure of oxygen, bar
STD	syngas to DME process
TPO	temperature programmed oxidation
Y_{DME}	yield of DME

catalyst is prepared with an excess of the acidic function, even when coke on the acidic phase is significant, the main cause of catalyst deactivation is coke deposition on CuO-ZnO metallic sites and on Al$_2$O$_3$, support of the metallic function. The difference in catalyst composition and, particularly, in the ratio between the metallic and acidic functions are relevant factors to compare deactivation results and its causes in the literature [16,24–27].

The presence of methoxy ions as intermediates is well known in the dehydration of methanol to DME [29] and in the transformation of both oxygenated compounds into hydrocarbons [30]. Furthermore, the degradation of these ions has been proposed as the main cause of coke deposition in the transformation of methanol into hydrocarbons [31]. Methoxy species are also considered as intermediate compounds in the ICI high temperature methanol synthesis [32]. Furthermore, the aforementioned hypotheses about the origin and deposition of coke are consistent with those appearing in the literature concerning the deactivation of bifunctional catalysts used in reactions performed in media of similar composition, such as the transformation of syngas into gasoline [33] and DME steam reforming [34].

A kinetic model for catalyst deactivation in a wide range of operating conditions has been established, whose main characteristics are: (i) the assumption that deactivation affects the methanol synthesis step; (ii) water in the reaction medium is of great importance for the attenuation of deactivation, since coke formation on the metallic function is reduced [35].

Nevertheless, the contribution of Cu sintering to catalyst deactivation should not be ignored. Sintering is considerable approximately above 300 °C [36], although the formation of spinels (CuO-ZnO in the case of CuO-ZnO/γ-Al$_2$O$_3$ catalyst) makes it possible to operate at higher temperature, since the stability of the metallic phase is improved [10]. However, sintering to be the cause of deactivation is explained in the literature by the loss of active Cu surface [37], although this result may be due to the deposition of coke on the metallic sites and on the interface between the metallic sites and the support. One of the aims of this work is to determine the maximum reaction temperature to avoid deactivation by sintering (irreversible) by studying catalyst performance in reaction–regeneration cycles, which is the more reliable method to establish the limits between reversible and irreversible deactivation.

In order to regenerate the catalyst, coke removal by combustion must be carried out without sintering the metallic phase. Therefore, the maximum combustion temperature and the composition of the comburent gas must be determined in order for the metallic sites to remain below this temperature during coke combustion. In this study the conditions for catalyst regeneration have been established, since they are a key factor for the viability of the STD process and scant attention has been paid in the literature.

2. Experimental

2.1. Catalyst

The CuO-ZnO-Al$_2$O$_3$ metallic function has been prepared by co-precipitating the corresponding metallic nitrates with Na$_2$CO$_3$ at pH 7.0 [38]. The γ-Al$_2$O$_3$ acid function has been prepared by the coprecipitation of a NaAlO$_2$ suspension with HCl at 70 °C until pH reaches a value of 9.0. The following steps are the aging of the catalyst at 70 °C for 1 h, filtering, washing, drying (at 20 °C and at 120 °C for 12 h each) and calcination (550 °C, 2 h). This function has low acid strength in order to minimize the transformation of methanol and DME into light olefins and heavy hydrocarbons, which may undergo degradation to produce coke.

CuO-ZnO-Al$_2$O$_3$/γ-Al$_2$O$_3$ bifunctional catalyst has been prepared by mixing the dry metallic function and the acid function in an aqueous solution, using a mass ratio of 2:1, which is the ratio that provides the best catalytic performance [39]. Thus, the deterioration of catalyst activity for the dehydration of methanol to DME due to the adsorption of water on γ-Al$_2$O$_3$ is avoided, and the shift of this equilibrium step is ensured. Furthermore, this mass ratio between the metallic function and the acid one is appropriate for ensuring that methanol synthesis is the limiting step, thus leading to a rapid transformation of methanol into DME. Subsequent to the mixing of metallic and acid functions, the suspension is centrifuged and the solid is washed, dried (in two steps, at 20 °C and 120 °C for 12 h each step) and calcined (300 °C, 6 h).

The Cu:Zn:Al atomic ratio determined by means of X-ray fluorescence (Philips Minipal PW4025) is 2.1:1.0:2.8. The metallic surface area, determined by N$_2$O chemisorption (in a Micromeritics Autochem 2920 coupled to a Pfeiffer Omnistar mass spectrometer), is 11.7 m^2 (g of catalyst)$^{-1}$. The physical properties, measured by N$_2$ adsorption–desorption (Micromeritics ASAP 2000) are: BET surface area, 125.3 m^2 g^{-1}; pore volume, 0.227 cm^3 g^{-1}, and average pore diameter, 74.5 Å.

By means of the thermogravimetric and calorimetric measurement of NH$_3$ adsorption at 150 °C (Setaram TG-DSC111 calorimeter coupled to a Pfeiffer Omnistar mass spectrometer) [40], a total acidity of 0.03 (mmol of NH$_3$) (g of catalyst)$^{-1}$ and an acidic strength of 100 kJ (mol of NH$_3$)$^{-1}$ have been determined, with a peak at 250 °C in the curve of temperature programmed desorption.

Prior to use, the bifunctional catalyst has been subjected to an equilibration treatment by oxidation-reduction in the reactor itself, which consists in exposing it to a H$_2$ stream diluted in He (10% of H$_2$) at 200 °C for 14 h and, subsequently, to a second stream (20% of H$_2$) at 300 °C for 1 h. This treatment was previously optimized and is aimed at the reduction of the CuO of the metallic function to Cu^0, which is the component of higher activity in the synthesis of methanol. The treatment is similar to that described in the literature for catalysts of similar composition [41].

2.2. Equipment and reaction conditions

The reaction equipment used (PID Eng. & Tech. Microactivity) is provided with a fixed bed, which allows for operating at high

temperatures and pressures. On-line product analysis has been carried out by means of a Varian CP-4900 gas micro-chromatograph. The reaction mixture is passed through several purifiers to eliminate possible traces of oxygen, water and iron carbonyl that may deactivate the catalyst.

Runs have been carried out feeding (H_2 + CO) under the following conditions: temperature, 250, 275, 325, and 375 °C; pressure, 20, 30 and 40 bar; space time, 8.4 and 12.8 (g of catalyst) h (mol of reactants)$^{-1}$; (H_2/CO) molar ratio in the feed, 2/1, 3/1 and 4/1; time on stream, 30 h; molar flowrate of reactants, 1 mmol (H_2 + CO) min^{-1}; catalyst particle size, 0.4 mm.

The micro-chromatograph is provided with three columns: (i) MS5 molecular sieve (10 m × 12 μm) for the separation of H_2, CO and CH_4; (ii) Porapak Q, PPQ (10 m × 20 μm) for the separation of CO_2, CH_4, C_2H_6, C_3H_8, C_4H_{10}, methanol, and DME; (iii) CPSil (8 m × 2 μm) for the separation of C_4–C_{10} fraction. The response factor of each compound has been determined by analysing mixtures of products of known composition.

2.3. Coke combustion

A conventional thermobalance (T.A. Instruments SDT 2960) coupled to a mass spectrometer (Thermostar from Balzers Instruments) has been used. The experimental procedure involves the following steps: (i) loading of the sample, passing a high purity He stream in order to remove air from the system; (ii) sweeping with He at 300 °C for 30 min; (iii) lowering sample temperature to 150 °C, and sweeping with streams of pure He and O_2–He (50%), with a flowrate of 30 cm^3 min^{-1} each, until constant values of the signals corresponding to the combustion products are obtained; (iv) heating at a rate of 5 °C min^{-1}, until coke combustion is completed.

The sweeping treatment prior to coke combustion is of great importance. The aim is the aging of the coke by homogeneizing its structure. Thus, cokes formed in the same process under different conditions have similar combustion kinetics after being aged [42,43]. Aging is important in order to use coke combustion kinetics in the design of the regeneration step of the process at industrial scale.

3. Results

3.1. Combustion of the coke of catalysts used under different conditions

Fig. 1 shows, as an example, the TPO curves of two samples of deactivated catalyst with different coke content, as a consequence of the different water/syngas molar ratio in the feed used in each run, 0.08 (Fig. 1a) and 0.20 (Fig. 1b). Runs have been performed under the following reaction conditions: 275 °C; 30 bar; H_2/CO molar ratio in the feed, 3/1; space time, 12.8 (g of catalyst) h (mol of reactants)$^{-1}$. Total coke amount on catalytic samples is 4.1 wt% and 1.2 wt%, respectively, as a result of the important role of water in the reaction medium in the attenuation of coke deposition [27].

TPO curves in Fig. 1 reveal the heterogeneous nature of coke, with two characteristic peaks corresponding to different coke location on the bifunctional catalyst. The carbonaceous material removed at low temperature, with a peak between 240 °C and 260 °C, is deposited on the CuO–ZnO metallic sites or on the interface between these sites and the Al_2O_3 support, so that its combustion is activated by the metallic sites. The fraction of coke which requires a higher temperature, between 330 °C and 380 °C, is deposited on the Al_2O_3 support and its combustion is not catalysed. This heterogeneity in coke combustion is characteristic of supported metallic catalysts [44,45] and bifunctional catalysts [46–49], in which the combustion of the coke deposited over the metal may start at temperatures above 150 °C [47,49], as shown in
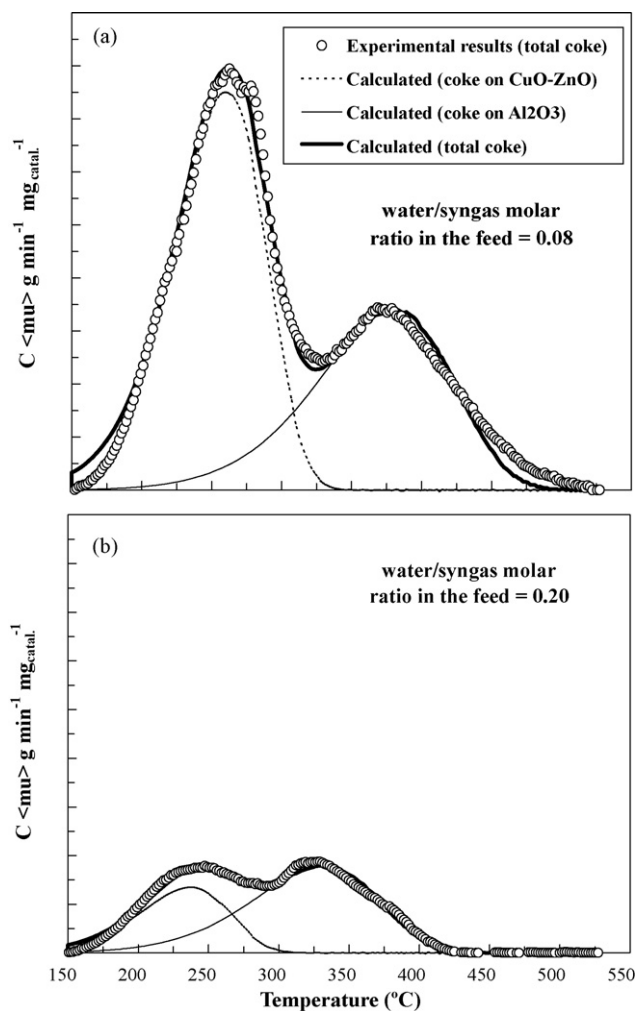

Fig. 1. Comparison between experimental results (points) and those calculated with the kinetic model (lines), corresponding to the combustion of coke formed in experiments with different water content in the feed. (Graph a) Water/syngas molar ratio 0.08. (Graph b) Water/syngas molar ratio 0.20. Reaction conditions: temperature, 275 °C; pressure, 30 bar; H_2/CO molar ratio in the feed, 3/1; space time, 12.8 (g of catalyst) h (mol of reactants)$^{-1}$.

Fig. 1. A similar circumstance of heterogeneity in coke combustion is observed for catalysts composed only of an acid function, but with bimodal pore structure, in which a more evolved coke (with a lower H/C ratio) is generated in the mesopores, whose combustion is slower than the less evolved coke (more hydrogenated) generated in the micropores [43,50].

The TPO curves of coke combustion are an effective tool for determining coke morphology, as well as its location within the catalyst. Although cokes of heterogeneous composition are identified, the kinetic models used to quantify coke combustion kinetics do not usually take into account this heterogeneity [51–54]. In this paper, the heterogeneity has been considered by establishing one kinetic equation for each coke fraction (fraction 1, coke fraction of fast combustion and fraction 2, that of slow combustion) with reaction order one for both oxygen and carbon, as it is frequently reported for cokes whose combustion takes place uniformly throughout the whole catalyst particle [55,56].

$$-\frac{dC_1}{dt} = k_1 P_{O_2} C_1 \tag{1}$$

$$-\frac{dC_2}{dt} = k_2 P_{O_2} C_2 \tag{2}$$

where k_1 and k_2 are the kinetic constants of combustion for both carbonaceous deposits, P_{O_2} is the partial pressure of oxygen, and C_1 and C_2 are the contents of the two coke fractions.

The effect of temperature on the kinetic constants has been taken into account by means of a reparameterized Arrhenius equation, considering a reference temperature of 250 °C:

$$k_i = k_{ref,i} \exp\left[\frac{-E_i}{R}\left(\frac{1}{T} - \frac{1}{523}\right)\right] \qquad (3)$$

where k_i and $k_{ref,i}$ are the kinetic constants for the combustion of i coke at T temperature and at the reference temperature (250 °C), respectively, and E_i is the activation energy corresponding to the combustion of each type of coke. The reparameterization of the Arrhenius equation by defining a kinetic constant based on a reference temperature eliminates the correlation between the activation energy and the preexponential factor in the kinetic calculation.

Deconvolution of TPO curves in order to identify the content of both coke fractions (C_1 and C_2) and the fitting of these contents to the kinetic equations for parameter calculation have been carried out using a programme written in MATLAB. Fig. 1 shows the TPO curves of both coke fractions, obtained as a result of the deconvolution.

Figs. 2–4 show the TPO curves of coke combustion for different values of reaction temperature, pressure and H_2/CO molar ratio in the feed, respectively, using a space time of 8.4 (g of catalyst) h (mol of reactants)$^{-1}$.

Table 1 lists the results of the kinetic parameters of coke combustion corresponding to Fig. 1, along with those corresponding to coke combustion in other operating conditions. The data of total coke content, also listed in Table 1, are consistent with the results of the evolution with time on stream of DME yield for different operating conditions [16,19,39]. In the same way, the results in Figs. 1–4 are consistent with the hypothesis of coke origin (C_1 fraction over the metallic function) and its growth in the Al_2O_3 support (C_2 fraction), which becomes more important as deactivation severity increases [27].

Regarding the values of the kinetic parameters of coke combustion (Table 1), activation energy is similar for both coke fractions, which supports the hypothesis that these fractions are related to the different location of coke, and not to the heterogeneity of its composition. The calculated values (around 60–70 kJ mol^{-1}) are similar to that obtained for metallic catalysts supported on Al_2O_3 [57]. The location of C_1 fraction in contact with the metallic sites explains the fact that the kinetic constant of its combustion is 7–26 times higher than that of the coke deposited on the Al_2O_3 support. This activation of coke combustion by the metallic sites is characteristic of the bifunctional catalysts [46–48,58]. The role of Cu as an oxidant of coke precursors and as a catalyst for their combustion is well accepted in the literature [59].

Figs. 1–4 evidence the important effect of the operating conditions on coke deposition. Fig. 1 shows that when water content in the feed increases from a water/syngas molar ratio of 0.08 (Fig. 1a) to 0.20 (Fig. 1b), the peak corresponding to coke deposited on the metallic function is much lower.

When reaction temperature is increased from 275 °C (Fig. 2a) to 325 °C (Fig. 2b), coke content decreases, which is explained by the fact that coke is generated by the degradation of oxygenated compounds (methanol and DME), whose concentration in the reaction medium decreases as temperature is increased, as a result of the thermodynamic limitation. It is observed that the decrease in coke content corresponds to the fraction deposited on the metallic function.

The effect of increasing coke content by pressure is very important (Fig. 3) and it mainly affects the carbonaceous material
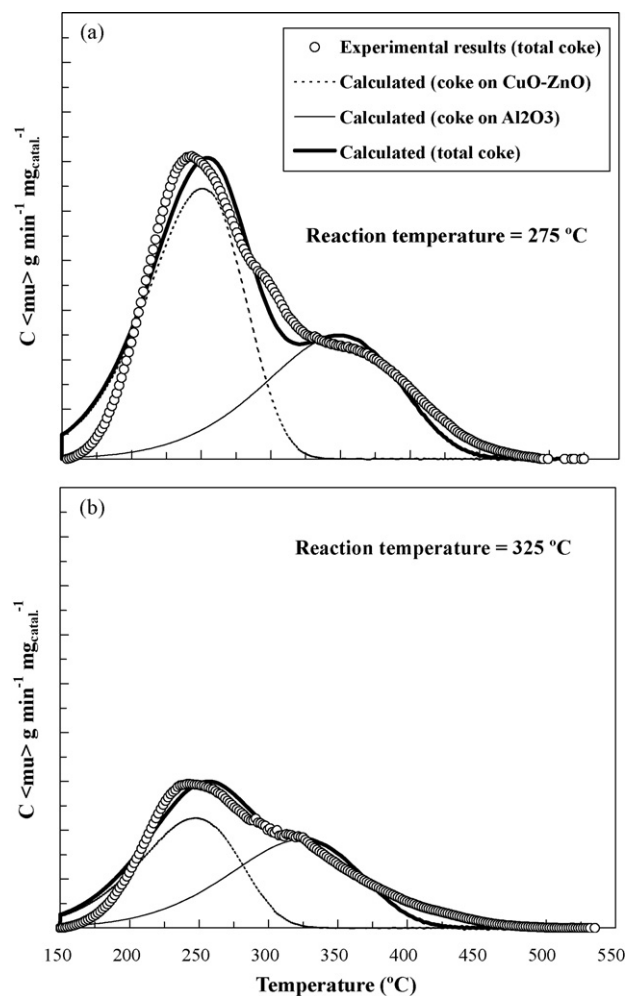

Fig. 2. Comparison between experimental results (points) and those calculated with the kinetic model (lines), corresponding to the combustion of the coke formed in runs at different reaction temperature. (Graph a) 275 °C. (Graph b) 325 °C. Reaction conditions: pressure, 30 bar; H_2/CO molar ratio in the feed, 4/1; space time, 8.4 (g of catalyst) h (mol of reactants)$^{-1}$.

deposited on the metallic function. It is also observed (Table 1) that, as pressure increases, the kinetic constant of combustion of both coke fractions becomes higher, which means a higher implication of the metallic function in the combustion of the coke generated at higher pressure.

H_2/CO molar ratio in the feed has a relevant effect, since when it is increased from 2/1 (Fig. 4a) to 3/1 (Fig. 4b) coke content increases significantly, due to the increase in DME yield. The highest DME yield is obtained for a H_2/CO molar ratio around 3/1 [39]. The fact of increasing H_2/CO molar ratio to 4/1 (Fig. 4c) affects the development of the coke fraction located on Al_2O_3 (peak at high temperature), which is explained by the lower DME yield, thus leading to an incipient growth of coke in this position.

Fig. 5 shows the compensation effect (also named isokinetic effect, theta rule or linear free energy relationship), which is characteristic of heterogeneous catalysis [60], as well as other combustion processes [61–63]. Two different linear relationships, corresponding to both coke fractions, are observed, which supports the hypothesis that the combustion phenomena of both fractions follow different mechanisms based on their different relationship with the metallic function. It must be noted that coke combustion mechanism is complex, given that it should account for the formation of reactive oxygen intermediates [64].
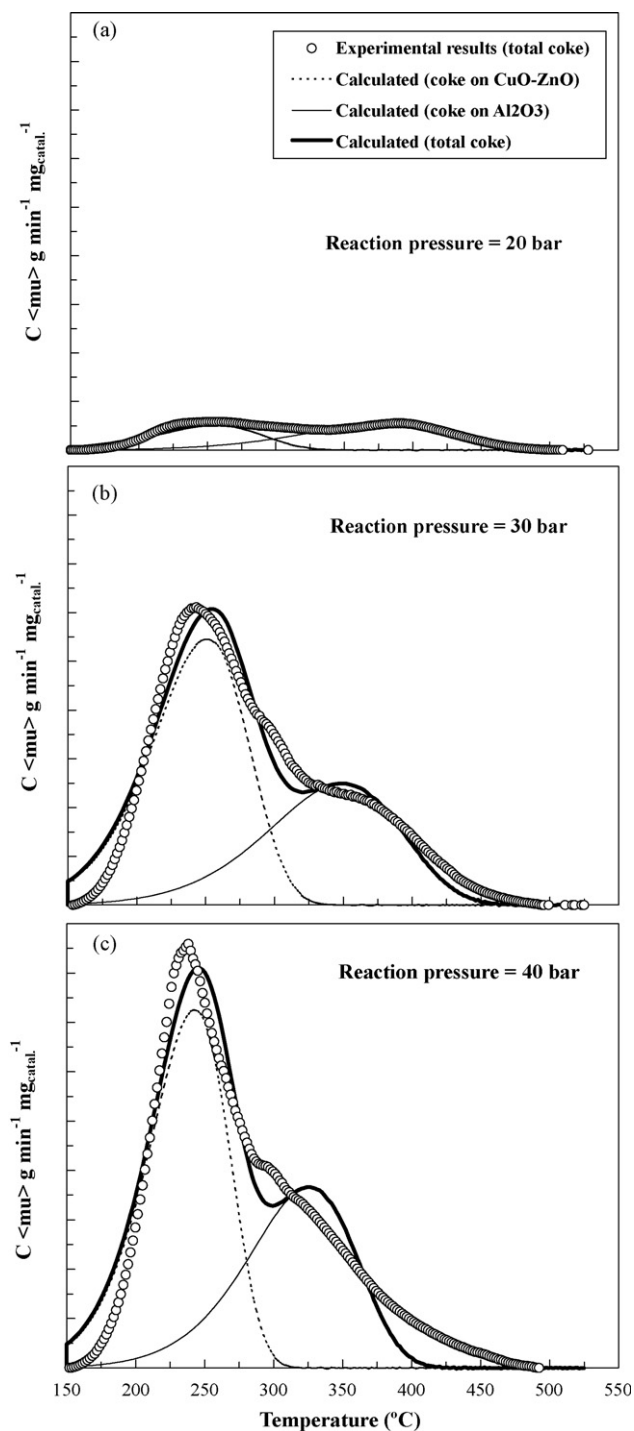
Fig. 3. Comparison between experimental results (points) and those calculated with the kinetic model (lines), corresponding to the combustion of the coke formed in runs at different pressure. (Graph a) 20 bar. (Graph b) 30 bar. (Graph c) 40 bar. Reaction conditions: temperature, 275 °C; H₂/CO molar ratio in the feed, 4/1; space time, 8.4 (g of catalyst) h (mol of reactants)⁻¹.
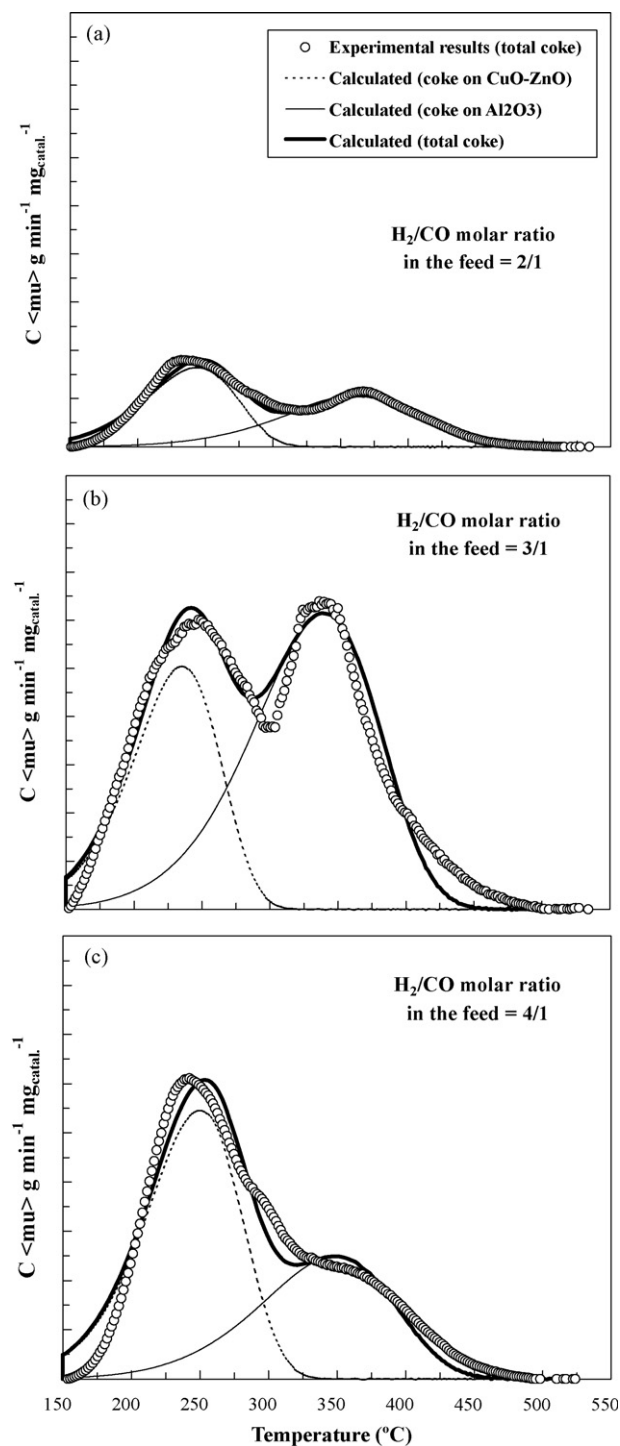
Fig. 4. Comparison between experimental results (points) and those calculated with the kinetic model (lines), corresponding to the combustion of the coke formed in runs with different H₂/CO molar ratio in the feed. (Graph a) H₂/CO 2/1. (Graph b) H₂/CO 3/1. (Graph c) H₂/CO 4/1. Reaction conditions: temperature, 275 °C; pressure, 30 bar; space time, 8.4 (g of catalyst) h (mol of reactants)⁻¹.

3.2. Operation in reaction–regeneration cycles

Reaction–regeneration cycles (up to 10 cycles) have been performed with the aim of: (i) determining the maximum reaction temperature to avoid the sintering of the metallic function (responsible for the irreversible deactivation) and (ii) establishing the maximum combustion temperature and the efficient comburent for the complete removal of coke (reversible deactivation),

in order for the kinetic performance of the catalyst to be fully recovered.

The reaction step has been carried out under the following conditions: 275 °C and 375 °C; 30 bar; H₂/CO molar ratio in the feed, 3/1; space time, 12.8 (g of catalyst) h (mol of reactants)⁻¹. Regeneration is performed in situ in the reactor, and prior to coke combustion step the catalyst bed is subjected to sweeping with N₂ for 1 h at the reaction temperature, with the aim of homogenizing

Table 1
Coke contents and kinetic parameters for the combustion of both coke fractions, under different operating conditions.

Water/ syngas molar ratio	Temperature (°C)	Pressure (bar)	H_2/CO molar ratio	Space time (g_{catal} h mol_{react}^{-1})	Coke content (wt%)	C_1 (wt%)	C_2 (wt%)	$k_{ref,1}$ ($bar^{-1} s^{-1}$)	$k_{ref,2}$ ($bar^{-1} s^{-1}$)	E_1 (kJ mol^{-1})	E_2 (kJ mol^{-1})
0.08	275	30	3/1	12.8	4.1	2.5	1.6	7.30×10^{-3}	2.83×10^{-4}	68.7	68.9
0.20	275	30	3/1	12.8	1.2	0.4	0.8	1.41×10^{-2}	8.20×10^{-4}	66.7	68.0
0	250	30	4/1	8.4	0.1	0.1	0	Kinetic parameters not calculable			
0	275	30	4/1	8.4	3.2	1.9	1.3	9.05×10^{-3}	6.77×10^{-4}	61.0	61.5
0	325	30	4/1	8.4	1.7	0.8	0.9	9.38×10^{-3}	1.26×10^{-3}	58.1	58.1
0	275	20	4/1	8.4	0.5	0.2	0.3	7.18×10^{-3}	3.75×10^{-4}	57.1	59.2
0	275	40	4/1	8.4	3.6	2.1	1.5	1.42×10^{-2}	1.02×10^{-3}	71.5	71.5
0	275	30	2/1	8.4	1.1	0.6	0.5	1.14×10^{-2}	4.72×10^{-4}	62.5	62.5
0	275	30	3/1	8.4	4.5	1.6	2.9	1.51×10^{-2}	8.30×10^{-4}	62.6	62.6

The kinetic constants have been calculated at a reference temperature of 250 °C.

the coke (by removing the volatile compounds of uncontrolled combustion) and obtain reproducible results [43,65,66]. This is the coke aging step detailed in the experimental part, which is also carried out prior to the combustion in thermobalance. Subsequently, there is a time period shorter than 2 h in each reaction step, in which syngas conversion and DME yield increase, until a stable oxidation-reduction level of maximum activity of the metallic phase is reached. Consequently, the results corresponding to the first 2 h of each reaction step have not been considered.

Fig. 6 shows the evolution with time on stream of DME yield in three reaction steps: first (corresponding to fresh catalyst), third (after two cycles of reaction–regeneration) and tenth (after nine cycles). The reaction step has been carried out at 275 °C and the regeneration has been conducted with air at 350 °C.

DME yield (Y_{DME}) has been calculated as the quotient between the molar flowrate of organic carbon in DME and the CO molar flowrate in the feed:

$$Y_{DME} = \frac{2n_{DME}}{(n_{CO})_0} 100 \qquad (4)$$

where n_{DME} is the molar flowrate of DME in the product stream and $(n_{CO})_0$ is the molar flowrate of CO in the feed.

The results of Fig. 6 are characteristic of catalysts which undergo sintering during the regeneration process and evidence that the initial DME yield decreases in each step by approximately one percentage unit, so that the accumulated decrease in DME yield in the tenth step compared to the first step is approximately ten percentage units. Although the temperature of 350 °C in the catalyst bed could be the cause of the sintering of the metallic

function, hot spots may also be generated on the metallic sites during the combustion of the coke deposited on these sites.

Fig. 7 shows the results of the evolution with time on stream of DME yield in first, third and tenth reaction steps. Reaction has been performed at 275 °C and regeneration has been carried out with O_2 diluted with He (5% of O_2) at 250 °C (Fig. 7a) and at 325 °C (Fig. 7b). It must be emphasized that the study of coke combustion in a thermobalance has revealed that the total coke amount deposited in the first reaction step is 5.5 wt%. It has been confirmed that coke is completely removed in 3 h at 325 °C. Nevertheless, combustion is incomplete at 250 °C, since a coke content corresponding to 5.1 wt% is burnt in 3 h, which evidences that this temperature is insufficient for the regeneration step.

Although the results of combustion in thermobalance reveal that coke combustion is incomplete at 250 °C using O_2 diluted to 5%, the catalyst recovers its initial activity when it is used in successive cycles of reaction–regeneration (Fig. 7a). A possible explanation to this phenomenon is that the fraction of coke deposited on the metallic function is completely removed, while part of the carbonaceous material located at the Al_2O_3 support remains unburnt. This remaining coke fraction is being accumulated in the successive cycles of reaction–regeneration, so that the decrease of DME yield with time on stream in the tenth reaction step is very fast. This result is typical of a coke rejuvenation process instead of a complete regeneration, and was already observed by Pieck et al. [44] in the regeneration of Pt-Re/Al_2O_3 catalysts.

When regeneration is conducted at 325 °C with diluted oxygen (Fig. 7b) the catalyst recovers its initial activity and mantains the kinetic performance for the time on stream studied (30 h).
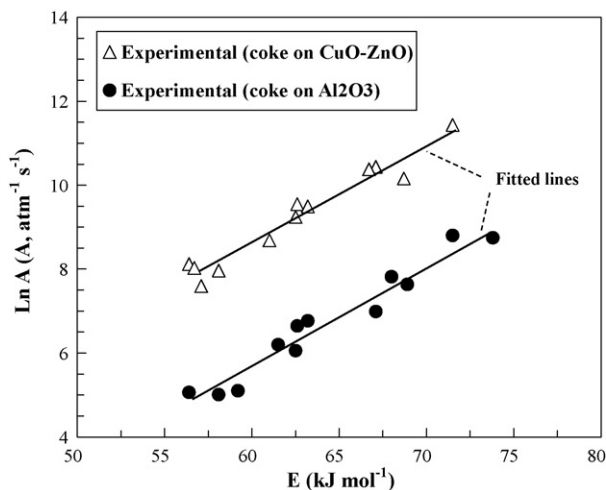
Fig. 5. Compensation effect for the kinetic parameters of combustion of both coke fractions.
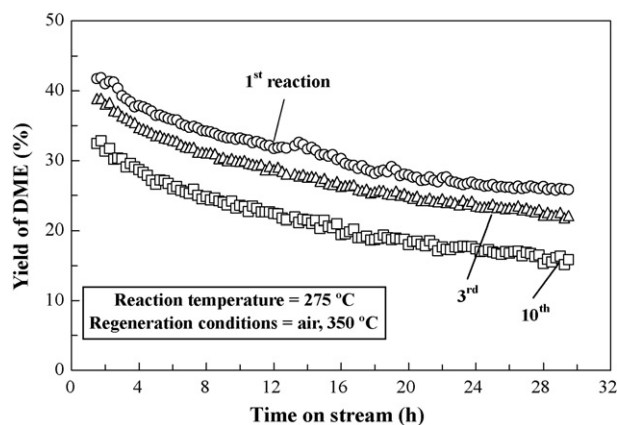
Fig. 6. Evolution with time on stream of DME yield in first, third and tenth reaction steps by operating in reaction–regeneration cycles. Reaction at 275 °C and regeneration at 350 °C with air.
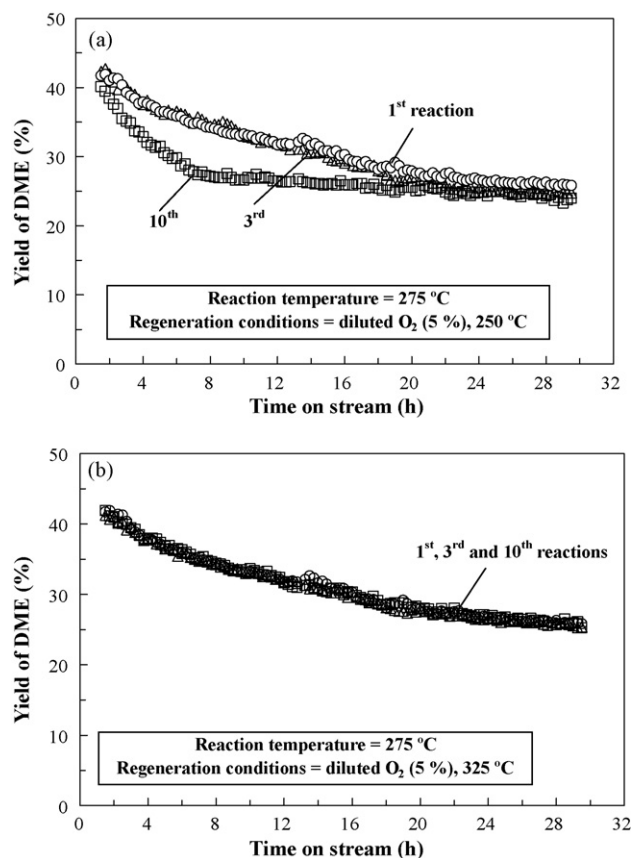
Fig. 9. Results of coke combustion in a thermobalance at different temperatures and using different comburents.

Fig. 9 shows the curves of CO_2 formation during coke combustion in thermobalance. The curves correspond to the results obtained using O_2 diluted with He (5% of O_2) at 325 °C and N_2O (5%) at 250 °C and 325 °C. A single peak is observed with diluted N_2O and at 250 °C, which corresponds to the combustion of part of the carbonaceous material deposited on the metallic function. This coke fraction (3.0 wt% by catalyst mass unit) is completely burnt-off at 325 °C. When diluted O_2 is used at 325 °C, all the coke is burnt-off (5.5 wt%).
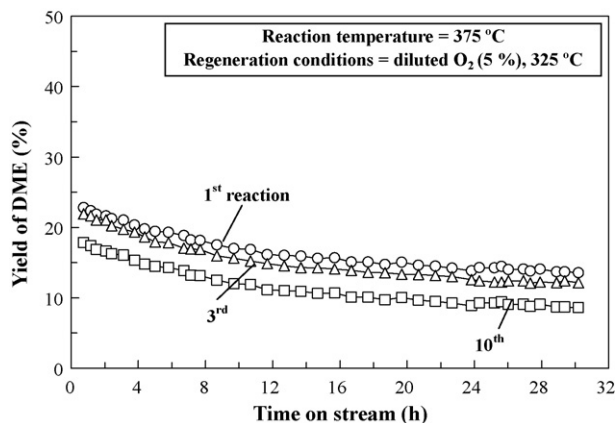

Fig. 7. Evolution with time on stream of DME yield in first, third and tenth reaction steps by operating in reaction–regeneration cycles. Reaction at 275 °C and regeneration with diluted O_2 (5%). (Graph a) Regeneration at 250 °C. (Graph b) Regeneration at 325 °C.

Furthermore, it has been proven that the reaction temperature must also be limited to avoid the sintering of CuO-ZnO spinel. Fig. 8 shows the results of reaction–regeneration cycles in which the regeneration step has been conducted at 325 °C with O_2 diluted with He, and the reaction has been performed at 375 °C. A slight decrease in catalyst activity is observed in the third reaction step, whereas this deterioration is significant in the tenth step.

The aforementioned situation of partial combustion of coke (when using diluted O_2 at 250 °C) also takes place when weaker oxidants such as N_2O and CO_2 are used in the regeneration step.

Fig. 10. Evolution with time on stream of DME yield in first, third and tenth reaction steps by operating in reaction–regeneration cycles. Reaction at 275 °C and regeneration with diluted N_2O (5%). (Graph a) Regeneration at 250 °C. (Graph b) Regeneration at 325 °C.

Fig. 8. Evolution with time on stream of DME yield in first, third and tenth reaction steps by operating in reaction–regeneration cycles. Reaction at 375 °C and regeneration at 325 °C with diluted O_2 (5%).
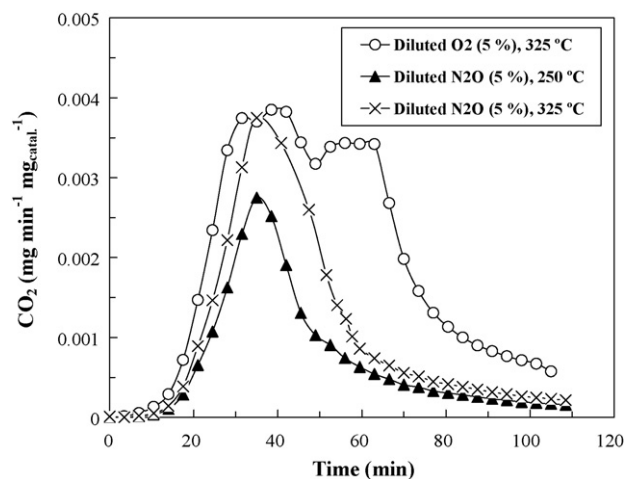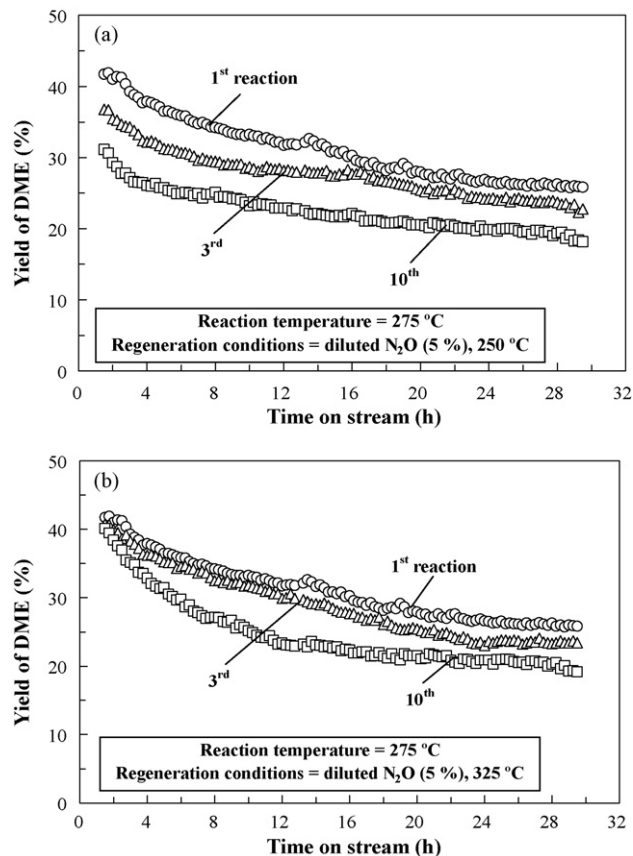
Table 2
BET surface area and metallic surface of the fresh catalyst and that regenerated after being used in reaction–regeneration cycles under different conditions in the reaction and regeneration steps.

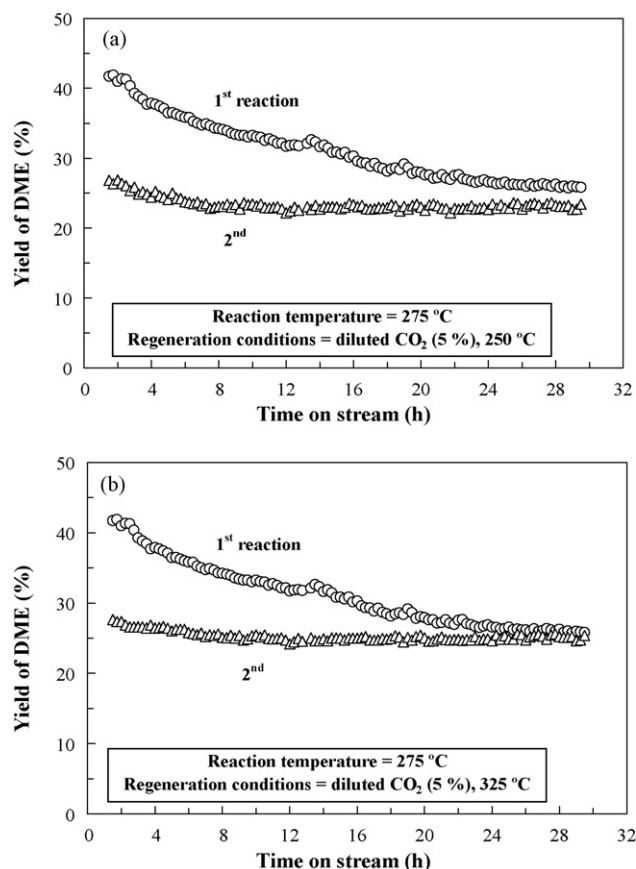| Reaction temperature (°C)	Comburent	Reaction–regeneration cycles	S_g BET (m^2 g$_{catal}^{-1}$)	Scu (m^2 g$_{catal}^{-1}$)
Fresh catalyst			125.3	11.7
275	Air, 350 °C	10	125.6	10.1
275	O$_2$ (5%), 250 °C	10	90.7	11.2
275	O$_2$ (5%), 325 °C	10	124.9	11.4
375	O$_2$ (5%), 325 °C	10	125.8	10.6
275	N$_2$O (5%), 250 °C	10	81.5	9.4
275	N$_2$O (5%), 325 °C	10	81.9	11.0
275	CO$_2$ (5%), 250 °C	2	80.3	7.9
275	CO$_2$ (5%), 325 °C	2	79.8	8.1

Fig. 11. Evolution with time on stream of DME yield in first and second reaction steps by operating in reaction–regeneration cycles. Reaction at 275 °C and regeneration with diluted CO$_2$ (5%). (Graph a) Regeneration at 250 °C. (Graph b) Regeneration at 325 °C.

The consequences of partial coke combustion by using N$_2$O as comburent are clearly observed when operating in reaction–regeneration cycles (Fig. 10). When regeneration is carried out at 250 °C (Fig. 10a), the catalyst does not fully recover its initial activity, owing to remaining coke that blocks the metallic sites. The catalyst is more rapidly deactivated in the following cycles of reaction–regeneration because coke is progressively accumulated. This progressive deactivation is attenuated when regeneration is conducted at 325 °C (Fig. 10b), as practically all the coke deposited on the metallic function is removed. The catalyst recovers its initial activity, but this situation only lasts for a short time on stream.

CO$_2$ diluted to 5% with He is not efficient to regenerate the catalyst, neither at 250 °C (Fig. 11a) nor 325 °C (Fig. 11b). The first regeneration step clearly shows that catalyst activity recovery is almost null.

3.3. Catalyst properties

Table 2 lists the values of BET surface area and the metallic surface of the fresh catalyst, as well as the catalyst in different regeneration states. It is observed that when the catalyst used in 10 cycles of reaction–regeneration is regenerated with air at 350 °C, the value of specific surface is recovered, since the coke deposited on the Al$_2$O$_3$ support of the metallic function is completely removed. Nonetheless, the value of the metallic surface is lower than that of the fresh catalyst, which confirms the hypothesis of Cu sintering when the regeneration step is conducted with air at 350 °C. The effect on the decrease of DME yield (Fig. 6) is relatively more significant than the decrease in the metallic surface. This result is explained by the fact that, due to the complex reaction scheme, deactivation directly affects the methanol synthesis step and indirectly the formation of DME [27,35].

When O$_2$ diluted with He (5% of O$_2$) is used in the regeneration step at 250 °C, most of the metallic surface is recovered but there is no recovery of BET surface area, which confirms the impossibility of removing most of the coke located at the Al$_2$O$_3$ support under these conditions. Nevertheless, when regeneration with diluted O$_2$ is conducted at 325 °C both the metallic and BET surface areas are recovered. It is also observed that, when the reaction is carried out at 375 °C, the catalyst undergoes sintering of the metallic function.

When diluted N$_2$O is used, the metallic surface is not fully recovered at 250 °C, while the recovery is almost complete at 325 °C. Nevertheless, BET surface area is not recovered in this case, since only the coke located at the metallic sites is removed, while the carbonaceous material deposited on the Al$_2$O$_3$ support remains unburnt.

Regeneration with CO$_2$ is not efficient for the recovery of neither the metallic surface nor BET surface area. This result and the aforementioned are consistent with the results of the experiments performed in reaction–regeneration cycles.

4. Conclusions

The combustion in thermobalance of the coke on the CuO-ZnO-Al$_2$O$_3$/γ-Al$_2$O$_3$ catalyst used in the synthesis of DME in one reaction step, after subjecting coke to an aging treatment, shows that coke is located at two positions and both coke fractions follow different combustion kinetics. Although the combustion of both fractions has a similar activation energy, the kinetic constant for the combustion of the first fraction (deposited on the metallic sites) is between 7 and 26 times higher than that for the remaining carbonaceous material, which is attributed to the catalytic activity of the metallic function.

O$_2$ diluted with He (with 5% of O$_2$) is efficient as a comburent in the regeneration by coke combustion of the catalyst deactivated in a fixed bed reactor. Using this oxidizing mixture at 325 °C, the carbonaceous material may completely be removed, avoiding excessive increases of temperature in the metallic sites. Regen-

erating the catalyst under these conditions and carrying out the reaction step below 325 °C, the catalyst does not undergo irreversible deactivation by Cu sintering, which allows using it in reaction–regeneration cycles with a repetitive kinetic behaviour. The calculated regeneration kinetics is suitable for its use in the design of this process.

A selective regeneration is observed in the fixed bed reactor with comburents for which coke combustion is very slow and even incomplete (diluted O_2, N_2O and CO_2) and at low temperature, which is due to the two coke fractions having different combustion kinetics. Accordingly, the metallic sites are regenerated first (leading to a recovery of the metallic surface of the catalyst) and subsequently the Al_2O_3 supporting the metallic sites (BET surface area is recovered). This result of selective regeneration is consistent with the results of selective coke combustion obtained in thermobalance.

Acknowledgements

References

[1] X.D. Peng, B.A. Toseland, P.J.A. Tijm, Chem. Eng. Sci. 54 (1999) 2787.
[2] X.D. Peng, A.W. Wang, B.A. Toseland, P.J.A. Tijm, Ind. Eng. Chem. Res. 38 (1999) 4381.
[3] T.A. Semelsberger, R.L. Borup, H.L. Greene, J. Power Sources 156 (2006) 497.
[4] C. Arcoumanis, C. Bae, R. Crookes, E. Kinoshita, Fuel 87 (2008) 1014.
[5] H.J. Kim, H.K. Suh, C.S. Lee, Energy Fuels 22 (2008) 2851.
[6] H.J. Kim, H.K. Suh, S.H. Park, C.S. Lee, Energy Fuels 22 (2008) 2091.
[7] J.Q. Chen, A. Bozzano, B. Glover, T. Fuglerud, S. Kvisle, Catal. Today 106 (2005) 103.
[8] T.A. Semelsberger, K.C. Ott, R.L. Borup, H.L. Greene, Appl. Catal. A 309 (2006) 210.
[9] Y.Z. Chen, Z.P. Shao, N.P. Xu, J. Natural Gas Chem. 17 (2008) 75.
[10] K. Faungnawakij, T. Fukunuga, R. Kikuchi, J. Catal. 256 (2008) 37.
[11] S.J. Park, D.W. Lee, C.Y. Yu, K.Y. Lee, K.H. Lee, Ind. Eng. Chem. Res. 47 (2008) 1416.
[12] S. Ahlgren, A. Baky, S. Bernesson, A. Nordberg, O. Noren, P.A. Hansson, Biosyst. Eng. 99 (2008) 145.
[13] J.L. Li, X.G. Zhang, T. Inui, Appl. Catal. A 147 (1996) 23.
[14] E.J. Kim, N.K. Park, G.B. Han, S.O. Ryu, T.J. Lee, Process Saf. Environ. Protect. 84 (2006) 469.
[15] D.S. Mao, W.M. Yang, J.C. Xia, B. Zhang, G.Z. Lu, J. Mol. Catal. A 250 (2006) 138.
[16] A.T. Aguayo, J. Ereña, I. Sierra, M. Olazar, J. Bilbao, Catal. Today 106 (2005) 265.
[17] A. Hadipour, M. Sohrabi, Chem. Eng. J. 137 (2008) 294.
[18] J.H. Kim, M.J. Park, S.J. Kim, O.S. Joo, J.D. Jung, Appl. Catal. A 264 (2004) 37.
[19] J. Ereña, R. Garoña, J.M. Arandes, A.T. Aguayo, J. Bilbao, Catal. Today 107–108 (2005) 467.
[20] D. Jin, B. Zhu, Z. Hou, J. Fei, H. Lou, X. Zheng, Fuel 86 (2007) 2707.
[21] S.H. Kang, J.W. Bae, K.W. Jun, H.S. Potdar, Catal. Commun. 9 (2008) 2035.
[22] G.R. Moradi, M. Nazari, F. Yaripour, Fuel Process. Technol. 89 (2008) 1287.
[23] D. Mao, J. Xia, Q. Chen, G. Lu, Catal. Commun. 10 (2009) 620.
[24] Y.S. Luan, H.Y. Xu, C.Y. Yu, W.Z. Li, S.F. Hou, Catal. Lett. 115 (2007) 23.
[25] F.S.R. Barbosa, V.S.O. Ruiz, J.L.F. Monteiro, J.R.R. De Avillez, L.E.P. Borges, L.G. Appel, Catal. Lett. 126 (2008) 173.
[26] D. Wang, Y. Tan, Y. Han, N. Tsubaki, J. Fuel Chem. Technol. 36 (2008) 171.
[27] J. Ereña, I. Sierra, M. Olazar, A.G. Gayubo, A.T. Aguayo, Ind. Eng. Chem. Res. 47 (2008) 2238.
[28] M. Guisnet, P. Magnoux, Appl. Catal. A 212 (2001) 83.
[29] W. Wang, M. Seiler, M. Hunger, J. Phys. Chem. B 105 (2001) 12553.
[30] P.L. Benito, A.G. Gayubo, A.T. Aguayo, M. Olazar, J. Bilbao, J. Chem. Tech. Biotechnol. 66 (1996) 183.
[31] A.T. Aguayo, A.G. Gayubo, R. Vivanco, A. Alonso, J. Bilbao, Ind. Eng. Chem. Res. 44 (2005) 7279.
[32] R. Yang, Y. Fu, Y. Zhang, N. Tsubaki, J. Catal. 228 (2004) 23.
[33] J. Ereña, J.M. Arandes, J. Bilbao, A.G. Gayubo, H.I. de Lasa, Chem. Eng. Sci. 55 (2000) 1845.
[34] T. Kawabata, H. Matsuoka, T. Shishido, D.L. Li, Y. Tian, T. Sano, K. Takehira, Appl. Catal. A 308 (2006) 82.
[35] I. Sierra, J. Ereña, A.T. Aguayo, M. Olazar, J. Bilbao, Ind. Eng. Chem. Res., in press, doi:10.1021/ie900978a.
[36] H.H. Kung, Catal. Today 11 (1992) 443.
[37] S.G. Lee, A. Sardesai, Top. Catal. 32 (2005) 197.
[38] J. Ereña, J.M. Arandes, R. Garoña, A.G. Gayubo, J. Bilbao, J. Chem. Tech. Biotechnol. 78 (2003) 161.
[39] J. Ereña, R. Garoña, J.M. Arandes, A.T. Aguayo, J. Bilbao, Int. J. Chem. Reactor Eng. 3 (2005) A44.
[40] A.T. Aguayo, A.G. Gayubo, R. Vivanco, M. Olazar, J. Bilbao, Appl. Catal. A 283 (2005) 197.
[41] D. Wang, Y. Han, Y. Tan, N. Tsubaki, Fuel Process. Technol. 90 (2009) 446.
[42] C. Royo, J.M. Perdices, A. Monzón, J. Santamaría, Ind. Eng. Chem. Res. 35 (1996) 1813.
[43] J.M. Ortega, A.G. Gayubo, A.T. Aguayo, P.L. Benito, J. Bilbao, Ind. Eng. Chem. Res. 36 (1997) 60.
[44] C.L. Pieck, C.A. Querini, J.A. Parera, Appl. Catal. A 165 (1997) 207.
[45] C.L. Pieck, C.R. Vera, C.A. Querini, J.A. Parera, Appl. Catal. A 278 (2005) 173.
[46] M. Larsson, M. Hultén, E.A. Blekkan, B. Andersson, J. Catal. 164 (1996) 44.
[47] N. Martin, M. Viniegra, E. Lima, G. Espinosa, Ind. Eng. Chem. Res. 43 (2004) 1206.
[48] N. Martin, M. Viniegra, R. Zarate, G. Espinosa, N. Batina, Catal. Today 107–108 (2005) 719.
[49] M.R. Jovanovic, P.S. Putanov, Appl. Catal. A 159 (1997) 1.
[50] A.T. Aguayo, A.G. Gayubo, A. Atutxa, B. Valle, J. Bilbao, Catal. Today 107–108 (2005) 410.
[51] J.M. Kanervo, A.O.I. Krause, J.R. Aittamaa, P.H. Hagelberg, K.J.T. Lipiäinen, I.H. Eilos, J.S. Hiltunen, V.M. Niemi, Chem. Eng. Sci. 56 (2001) 1221.
[52] V.J. Fernandes Jr., A.S. Araujo, M.E. Madruga, L.F. Nicolini, Thermochim. Acta 392–393 (2002) 63.
[53] C. Kern, A. Jess, Chem. Eng. Sci. 60 (2005) 4249.
[54] T.J. Keskitalo, K.J.T. Lipiäinen, A.O.I. Krause, Chem. Eng. J. 120 (2006) 63.
[55] V.D. Dimitriadis, A.A. Lappas, I.A. Vasalos, Fuel 77 (1998) 1377.
[56] D. Ma, D. Wang, L. Su, Y. Shu, Y. Xu, X. Bao, J. Catal. 208 (2002) 260.
[57] K.M. Hardiman, C.G. Cooper, A.A. Adesina, R. Lange, Chem. Eng. Sci. 61 (2006) 2565.
[58] C. Royo, J. Santamaría, A. Monzón, Thermochim. Acta 274 (1996) 249.
[59] A.P. Antunes, M.F. Ribeiro, J.M. Silva, F.R. Ribeiro, P. Magnoux, M. Guisnet, Appl. Catal. B 33 (2001) 149.
[60] A. Corma, F. Llopis, J.B. Monton, S. Weller, J. Catal. 142 (1993) 97.
[61] N. Liu, R. Zong, L. Shu, J. Zhou, W. Fan, J. Appl. Polym. Sci. 89 (2003) 135.
[62] A.H. Osman, A.A.M. Aly, M.A. El-Mottaleb, G.A.H. Gouda, Bull. Korean Chem. Soc. 25 (2004) 45.
[63] A. Mianowski, R. Bigda, V. Zymla, J. Therm. Anal. Calorim. 84 (2006) 563.
[64] T.J. Keskitalo, K.J.T. Lipiäinen, A.O.I. Krause, Ind. Eng. Chem. Res. 45 (2006) 6458.
[65] P.L. Benito, A.T. Aguayo, A.G. Gayubo, J. Bilbao, Ind. Eng. Chem. Res. 35 (1996) 2177.
[66] P. Magnoux, H.S. Cerqueira, M. Guisnet, Appl. Catal. A 235 (2002) 93.